

Creep analysis of CFT columns subjected to eccentric compression loads

Bing Han, Yuan-feng Wang*, Qian Wang and Dian-jie Zhang

School of Civil Engineering, Beijing Jiaotong University, Beijing, China

(Received July 7, 2011, Revised May 31, 2012, Accepted September 19, 2012)

Abstract. By considering the creep characteristics of concrete core under eccentric compression, a creep model of concrete filled steel tubes (CFT) columns under eccentric compressive loads is proposed based on the concrete creep model B3. In this proposed model, a discrete element method is introduced to transform the eccentric loading into axial loading. The validity of the model is verified by comparing the predicting results with the published creep experiments results on CFT specimens under compressive loading, together with the predicting values based on other concrete creep models, such as ACI209, CEB90, GL2000 and elastic continuation and plastic flow theory. By using the proposed model, a parameters study is carried out to analysis the effects of practical design parameters, such as concrete mix (e.g. water to cement ratio, aggregate to cement ratio), steel ratio and eccentricity ratio, on the creep of CFT columns under eccentric compressive loading.

Keywords: concrete filled steel tubes; creep; eccentric compression; eccentricity ratio; model B3

1. Introduction

Due to many favorable performances, concrete filled steel tubes (CFT) structures have been widely adopted in bridges, high-rise buildings, and super high-rise buildings. Most research so far is focused on the short-term static or dynamic performances, while its time-dependent behavior research is relatively deficient. However, creep is considered as having great impact on reduction of concrete strength and initial elastic modulus, besides cumulative creep deformation can lead to differential shortening and even distortion of CFT columns, as a result, research in creep of CFT columns is quite important.

Creep of CFT columns is considerable different from that of ordinary concrete columns, which can be shown in several aspects, as follows (Naguib and Mirmiran 2003):

- (1) Little humidity changes are taken place in concrete core due to confinement of the tube, therefore drying creep and shrinkage strains are significantly lower in CFT.
- (2) Confinement pressure of concrete offered by the tube reduces lateral expansion of concrete core. The multi-stress effect prevents the concrete from creep freely in axial direction.
- (3) Stress transfer may occur between steel tube and concrete, which leads to stress relaxation of concrete core, and further lowering its creep.

*Corresponding author, Professor, E-mail: cyfwang@bjtu.edu.cn

(4) Because of the stress relaxation in concrete, stress in steel tube and concrete may vary over time, even though the load is remain as a constant. The variation should be taken into account in creep analysis.

The phenomena of creep and shrinkage of CFT was first discovered by Furlong in an experiment in 1967 (Furlong 1967). The experiment of Furlong (Furlong 1967) showed that though effect of creep was mitigated due to the existence of steel confinement, the creep had an influential effect on long-term behavior of CFT members. Hereafter, further investigations into CFT creep were conducted, but investigations into creep of CFT columns under eccentrically compressive loads are relatively less than that of CFT members under axial loads (Nakai *et al.* 1991, Ichinose *et al.* 2001, Uy 2001, Naguib and Mirmiran 2003, Han *et al.* 2004, Gajalakshmi *et al.* 2011, Wang *et al.* 2008).

Tan Su-jie *et al.* (Tan and Qi 1987) studied mechanical behaviors of circular CFT members by conducting creep experiments under eccentrically compressive loading during 1983 ~ 1984. There were 16 specimens of the columns, with different steel ratio, eccentricity ratio, and load ratio (0.63 ~ 1.13). Based on the experiments, the authors analyzed the development tendency of the creep of CFT members. All the specimens were loaded increasingly till breakdown after creep tests. Comparing those no creep occurred, the authors found that whatever the load ratio was, creep did not have much influence on load capacity of members.

Morino *et al.* (Morino *et al.* 1996) performed creep tests of square CFT columns under eccentrically compressive loading, with different eccentricity and so on. The creep coefficient and elastic modulus reduction coefficient of each specimen were calculated after the tests, and values of the two coefficients were found to be lower than that of concrete reinforcement members. Based on the tests, equations of creep strains were developed by means of least-square fitting. However, just a few factors were involved in the equation, so that the method could not be spread widely.

So far, several creep prediction models of CFT members have been developed using different factors by many researchers (Wang *et al.* 2008). However, these proposed models do not reflect characteristics of CFT mechanics and creep strains under eccentric compression loads well, and factors considered in the models are not complete as well. In practice, most of members are under eccentric compression loads rather than compression loads. Some researchers have demonstrated that the creep had significantly effects on behavior of CFT members and structures under eccentric loads (Wang and Han 2007, Shrestha and Chen 2011). Therefore, more theoretical and experimental work should be done in these aspects.

There are many statements about explanation of concrete creep phenomena, such as aging theory, ECPF theory, however, none of the theories can clarify the phenomena of concrete creep reasonably. The mechanism of concrete creep is thus unsolved yet.

Bazant (Bazant and Murphy 1995) developed model B3 of concrete creep and shrinkage estimation in 1995, on the base of solidification theory (Bazant and Prasanna 1989a, 1989b). Comparing with other models (ACI209, CEB90, GL2000), the Model B3 needs more parameters including water to cement ratio and aggregate to cement ratio of concrete. Through analysis of some documents, the Model B3 is proved to have clear theoretical foundation and good agreement with experimental work (Lam 2002, Rajeev *et al.* 2007), so it is reasonable to use the model B3 in creep analysis of CFT columns.

In this paper, a creep computation model for CFT columns under eccentric compressive loading is developed based on the model B3, which adheres to microscopic mechanism of concrete creep and considers creep characteristics of the concrete core under eccentric loading. In this model, a

discrete element method is introduced to transform the eccentric loading into the axial loading. The validity of the model is verified by comparing the predicted results with the published creep experiments results on CFT specimens, together with the predicting values based on other concrete creep models, such as ACI209, CEB90, GL2000 and ECPF theory. By using the proposed model, a parameters study is carried out to analyze the effects of practical design parameters, like concrete mixture (e.g. water to cement ratio (w/c), aggregate to cement ratio (a/c)), steel ratio (A_s/A_c) and eccentricity ratio (e), on creep of CFT column under eccentric compressive loading.

2. Creep calculation of CFT columns under eccentric compressive loading

2.1 Model B3

Creep is divided into two parts, basic creep and drying creep in Model B3 (Bazant and Murphy 1995), as

$$C(t, t', t_0) = C(t, t) + C_d(t, t', t_0) \quad (1)$$

where $C_0(t, t')$ — basic creep compliance;

$C_d(t, t', t_0)$ — drying creep compliance;

t — age of concrete;

t' — age of concrete at loading;

t_0 — age of concrete when drying begins (only when $t_0 \leq t'$);

(1) Basic creep compliance $C_0(t, t')$

Basic creep compliance is defined by its time rate

$$\dot{C}_0(t, t') = \frac{n(q_2 t^{-m} + q_3)}{(t - t') + (t - t')^{1-n}} + \frac{q_4}{t} \quad (2)$$

where q_2 — representing aging viscoelastic compliance, $q_2 = 451.1c^{0.5}(f_c)^{-0.9}$;

q_3 — representing non-aging viscoelastic compliance, $q_3 = 0.29(w/c)^{0.4} q_2$;

q_4 — representing flow compliance, $q_4 = 0.14(a/c)^{-0.7}$;

f_c — mean 28-day standard cylinder compression strength;

m, n — constants, $m = 0.5, n = 0.1$.

By integrating (2), we get

$$C_0(t, t') = q_2 Q(t, t') + q_3 \ln[1 + (t - t')^n] + q_4 \ln\left(\frac{t}{t'}\right) \quad (3)$$

where $Q(t, t')$ is a double integral and can be obtained from the following formula,

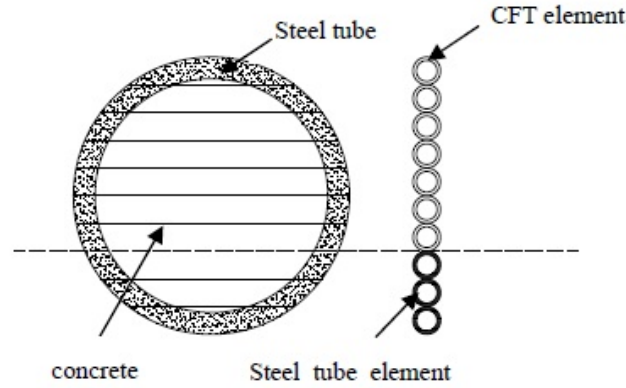


Fig. 1 Discretization of sections

$$\dot{Q}(t, t') = Q_f(t') \left[1 + \left(\frac{Q_f(t')}{Z(t, t')} \right)^{r(t')} \right]^{-1/r(t')} \quad (4)$$

(2) Drying creep compliance $C_d(t, t', t_0)$

$$C_d(t, t', t_0) = q_5 \{ \exp[-8H(t)] - \exp[-8H(t_0)] \}^{1/2}, t_0 = \max(t', t_0) \quad (5)$$

where $q_5 = 7.57 \times 10^5 f_c^{-1} \varepsilon_{sh\infty}^{-0.6}$;

$$H(t) = 1 - (1 - h)S(t);$$

$$S(t) = \tanh \left(\frac{t - t_0}{\tau_{sh}} \right)^{1/2}.$$

2.2 Creep calculation of CFT columns under eccentric compressive loading

2.2.1 Initial stress calculation

Initial stress calculation are based on following assumptions (Naguib and Mirmiran 2002): (a) the members' cross sections remain plain after loading, (b) perfect bond is assumed between steel tube and concrete and (c) contribution of concrete in torsion zone is neglected.

As shown in Fig. 1, the whole member is transformed into a series of solid CFT elements in compression above neutral axis and hollow steel tube elements in tension below neutral axis. Axial force in each element can be determined by stress and area of the element. A confinement model suggested by Ahmad and Shah (Ahmad and Shah 1982) is adopted as the concrete stress-strain model. Taking account strain compatibility into the model, the flexural analysis can be simplified into an axial analysis for each element.

The detailed calculation process is as follows:

- (1) The member is discretized, geometric properties are constructed, and depth of neutral axis and curvature are assumed.
- (2) Concrete strain at the top is ascertained by the depth of neutral axis and curvature; The strain in each element is determined according to the linear strain profile.
- (3) Using the model developed by Ahmad and Shah (Ahmad and Shah 1982), concrete stress in each element is calculated, and stress of steel tube in each element is obtained by steel elastic modulus and element strain.
- (4) Axial force and moment in each element are calculated.
- (5) The axial forces and moments are summed over the whole section. The results are compared with external axial load and moment. If there were deviation between them, the depth of neutral axis and curvature should be adjusted.
- (6) Steps 1-5 are repeated, till the convergence is achieved. Then, the depth of neutral axis and curvature are ascertained, and concrete stress at the top is thought as the initial stress.

2.2.2 Confinement stress

As stress distribution on the section is uneven, distribution of confinement stress is non-uniform for columns under eccentrically loading (Neville *et al.* 1983). Therefore, different from CFT members under axial loads, concrete core of CFT columns under eccentric compression loads is under triaxial stress with different confinement stress. According to Hook's law, confinement stress in radial direction can be written as

$$p = q\sigma_{c1} \tag{6}$$

in which,
$$q = \frac{n - \frac{n(1 + \mu_c)}{1 + \mu_s} - n\mu_c^2 + \mu_s\mu_c \frac{n(1 + \mu_c)}{1 + \mu_s}}{-\frac{2}{\alpha}\mu_c + \mu_c\mu_s \frac{n(1 + \mu_c)}{1 + \mu_s} + n\mu_c + \frac{2}{\alpha}\mu_s - \frac{n(1 + \mu_c)}{1 + \mu_s} + n\mu_c^2}$$

Confinement stress in hoop direction p_1 can be written as

$$p_1 = q_1\sigma_{c1} \tag{7}$$

in which,
$$q_1 = \frac{(n - \frac{n(1 + \mu_c)}{1 + \mu_s}) - (n\mu_c + \frac{2}{\alpha}\mu_s - \frac{n(1 + \mu_c)}{1 + \mu_s})q}{n\mu_c}.$$

2.2.3 Creep analysis

Fig. 2 shows stress distribution of CFT columns under eccentric compressive loading. ϵ_{sc} is total strain of concrete core where compression stress is maximum on the section; ϵ_{sc}^c is creep strain of concrete core where compression stress is maximum on the section; ϵ_c^c is plain concrete creep where compression stress is maximum on the section; ϵ_{sc}' is

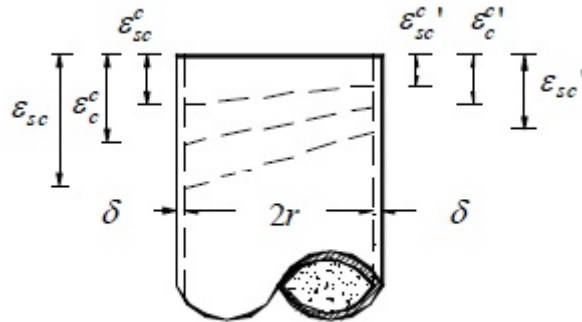


Fig. 2 Strain distribution of columns under eccentric compressive loading

minimum total strain of the section; $\epsilon_{sc}^{c'}$ is minimum creep strain of the section; $\epsilon_c^{c'}$ is creep of plain concrete where total strain of the section is minimum; r is radius of concrete core; δ is thickness of steel tube.

When stress redistribution occurs during creep, the changing of internal force and stress of concrete core is assumed to be N_c^c , σ_c^c respectively, and the changing of internal force and stress of steel tube is N_s^c , σ_s^c respectively. Therefore

$$N_s^c + N_c^c = 0 \tag{8}$$

$$\sigma_c^c = N_c^c \left(\frac{1}{A_c} + \frac{er}{I_c} \right) \tag{9}$$

$$\sigma_s^c = N_s^c \left(\frac{1}{A_s} + \frac{er}{I_s} \right) \tag{10}$$

The strain change of concrete core for CFTs during creep is

$$\epsilon_c^c = \sigma_{c1} c_1 \tag{11}$$

where, $\sigma_{c1} = \sigma_{c0} + \sigma_{c1}^c$, σ_{c0} can be calculated from the formula in 2.2.1;

σ_{c1}^c —stress change of concrete core during creep;

c_1 —axial creep compliance of concrete core, $c_1 = c(1 - \mu_{cp,1}(q_1 + q))$;

$\mu_{cp,1}$ is effective creep poisson of concrete in axial direction. See ref. (Neville *et al.* 1983);

c_2 —radial creep compliance of concrete core, $c_2 = c(1 - \mu_{cp,2}(\frac{q_1}{q} + \frac{1}{q}))$;

$\mu_{cp,2}$ is effective creep poisson of concrete in radial direction.

According to strain compatibility of concrete core and steel tube in axial and radial direction, we can have

$$\sigma_{c1}^c = - \frac{E_s c_1 + \frac{qc_2 E_s}{2\mu_s} \frac{2}{\alpha} \mu_s}{\frac{1}{\gamma} + E_s c_1 - \frac{2\mu_s}{\alpha} \frac{\mu_s}{\gamma} - qc_2 E_s} \sigma_{c0} \quad (12)$$

Substituting (12) into (11), we obtain creep calculation formula of CFT columns under eccentric compressive loading.

2.2.4 Creep calculation process of CFT columns under eccentric compressive loading

The creep calculation process of CFT columns under eccentric compressive loading is shown as in Fig. 3.

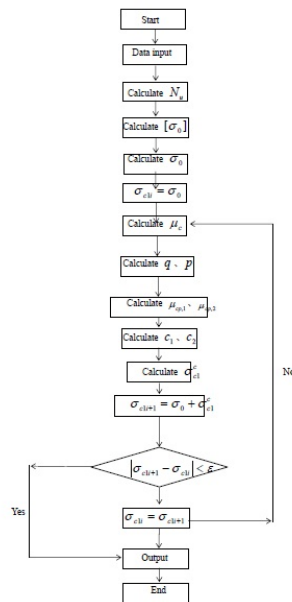


Fig. 3 Creep calculation process

2.2.5 Validation of the proposed creep prediction model

Three specimens from the experiment (Han *et al.* 2004) have been selected to verify the creep prediction model presented in the paper. Parameters related to the specimens and materials can be seen in Tables 1-3. To compare the predicted results of creep, model B3 is contrasted with other concrete creep model, such as ACI209, CEB90, GL2000 model, ECPF theory. Comparison results of creep obtained from these models are shown in Fig. 4.

Table 1 Experiment parameters (Group 1)

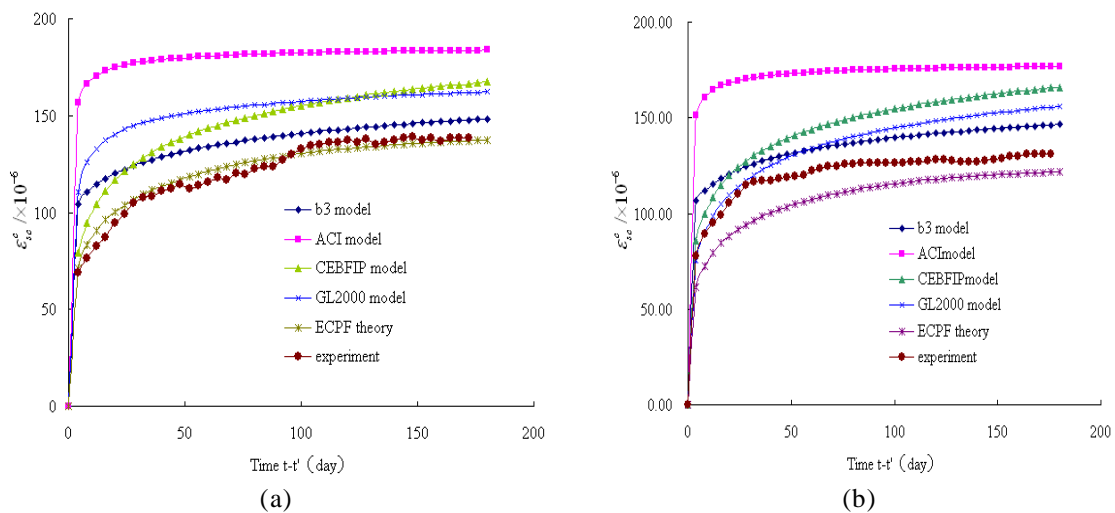
Steel tube outside diameter (mm)	Steel tube thickness (mm)	Specimen length (mm)	f_y (N/mm ²)	f_{ck} (N/mm ²)	Steel ratio	Eccentricity (mm)	Axial load (kN)
114	4.6	450	331.73	33.6	0.1833	21.35	275.99

Table 2 Experiment parameters (Group2)

Steel tube outside diameter (mm)	Steel tube thickness (mm)	Specime n length (mm)	f_y (N/mm ²)	f_{ck} (N/mm ²)	Steel ratio	Eccentricity (mm)	Axial load (kN)
114	4.69	450	331.73	33.6	0.1851	22.8	315.33

Table 3 Experiment parameters (Group3)

Steel tube outside diameter (mm)	Steel tube thickness (mm)	Specime n length (mm)	f_y (N/mm ²)	f_{ck} (N/mm ²)	Steel ratio	Eccentricity (mm)	Axial load (kN)
109.64	1.82	450	331.73	33.6	0.0686	21.1	312.29



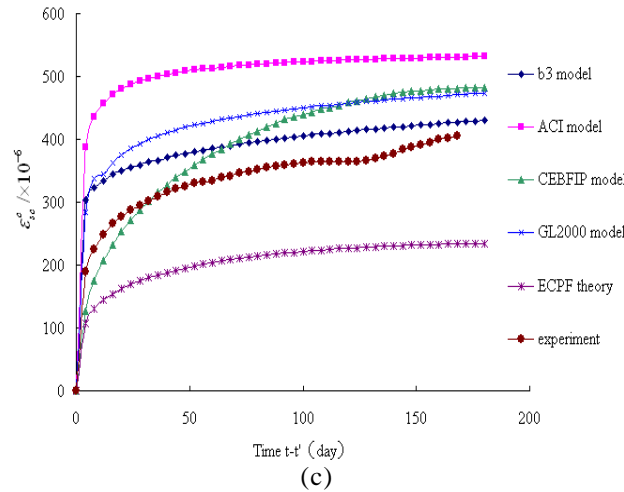


Fig. 4 Comparison of CFT creep prediction models

As shown from Figs. 4a-4c, the proposed model, ACI209, CEB-FIP and GL2000 model all overestimate creep in the CFT columns. Using different concrete creep models, matching degrees are non-uniform. From Figs. 4(a)-(c), we find that creep based on ACI model rise sharply in first 50 days, while stay stable after that. For three specimens, creep values obtained by this model are higher than experiments by 78%, 54% and 70% respectively in the first 50 days, while higher than experiments by 34%, 37% and 44% after the creep is stable.

Creep predicted by CEB-FIP and GL2000 does not still stabilize after 180 days, creep values based on CEB-FIP model is even bigger. Predicted results of the two models are higher than the experiments by 15%-20%. When creep in first 100 days are predicted, great difference occurs in the theoretical analysis of specimen 1 and 3 using the two models, maximum of which can reach to 50%. For specimen 1 and 3, difference between the theoretical analysis and experiments is only 21% and 10% respectively, while there is a gap of 32% and 29% respectively between the calculation results based on GL2000 and experiments of specimen 1 and 3. For specimen 2, the theoretical results based on the two models are almost the same in the first 100 days, higher than experiments by 18% and 10% respectively.

Also shown from Figs. 4(a)-(c) are the creep strains calculated by using ECPF theory. A good agreement is noted in the trend of creep curve of specimen 1, and difference is no more than 5%. For specimen 2, deviation between the calculation and experiments is about 12% in the first 100 days, however, different from other concrete creep models, the creep results using ECPF theory is lower than the experiments; while gap in later 80 days is within 8%. For specimen 3, also the predicted creep is lower than the experiment, and average difference between the calculation and experiment is up to 40%.

In the experiment for specimen 1, the calculation results based on Model B3 is averagely higher than experiment by 15% in the first 100 days, while after that, difference between the theoretical results and experiment is only 5%. For specimen 2, the predicted results and the experiments are close in the first 70 days, with a difference of 10%; while the difference varies to 14% afterwards. For specimen 3, trends of the theoretical and experimental curves are in a good agreement, and difference of the two is 11%. From the previous analysis, we see that the prediction results from present study based on Model B3 are relatively stable, and differences between the theoretical and

experimental curves are 10% approximately.

3. Parameter study

Factors that influence CFT creep can be divided into internal factors and external factors. By using the model proposed above, six examples are analyzed according to different effecting factors on creep of the CFT columns.

3.1 Internal factors

The internal factors mainly refer to the factors that lie in concrete core themselves, such as concrete mix proportion and so on. Effect of water to cement ratio and aggregate to cement ratio on CFT creep is presented in the paper. Two examples below are used to analysis effects of the

Table 4 Details of CFT columns

Steel tube outside diameter (mm)	Steel tube thickness (mm)	Specimen length (mm)	f_y (N/mm ²)	Steel ratio	Eccentricity (mm)	Axial load (kN)
120	4.0	450	315	0.148	16.8	300.0

Table 5 Parameters of concrete materials

Parameters Examples	w/c	a/c
1	0.30	6.0
	0.50	
2	0.35	4.0
		7.0
		10.0

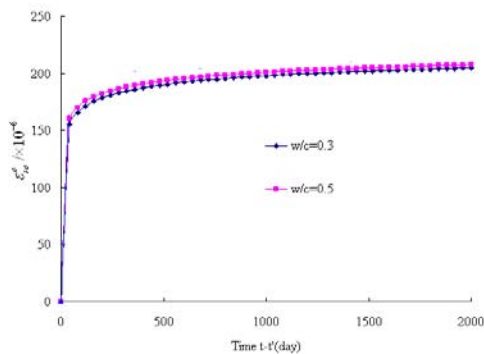


Fig. 5 Influence curves of water to cement ratio (example 1)

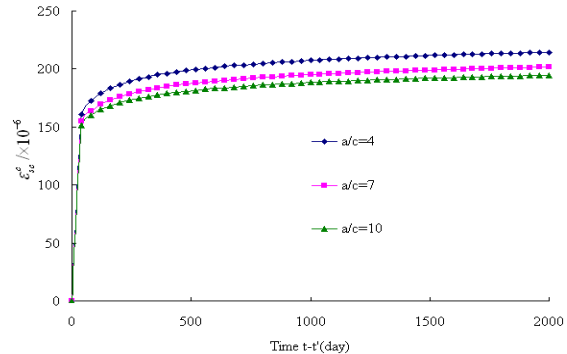


Fig. 6 Influence curves of aggregate to cement ratio (example 2)

internal factors. Dimension, axial load, eccentricity ratio and steel strength are the same for the examples, all of which are shown in Table 4. Concrete material parameters of each example are shown in Table 5.

Figs. 5-6 shows creep curves of the CFT columns with different water to cement ratio and aggregate to cement ratio when other parameters are the same. From Figs. 5-6, following conclusions have been drawn:

(1) Creep of CFT members decrease as water to cement ratio reduces. Creep will drop by 1.4% as water to cement ratio reduces from 0.5 to 0.3.

(2) Creep of CFT increases when aggregate to cement ratio of concrete core drops. When aggregate to cement ratio changes from 10.0 to 4.0, creep strains increase by 10.1%.

From the above analysis, effects of the two internal factors on creep of the CFT members are not as remarkable as that on creep of other concrete members. It is possible that the strong restriction effects of steel on concrete core make the deformation of the members insensitive to changes of creep due to various internal factors. However, controlling water to cement ratio and aggregate to cement ratio is still easy way to weaken creep effects on CFT columns in practice.

3.2 External factors

External factors mainly refer to concrete age at loading, load duration, steel ratio and so on. Effects of steel ratio, eccentricity, axial load and concrete age at loading on CFT creep are discussed in the paper through four examples.

Table 6(a) Details of CFT columns (example 3)

Steel tube outside diameter (mm)	Specimen length (mm)	f_y (N/mm ²)	f_{ck} (N/mm ²)	Eccentricity (mm)	Axial load (kN)	Age at loading (day)
120	450	315	26.8	16.8	300.0	28

Table 6(b) Details of CFT columns (example 4)

Steel tube outside diameter (mm)	Specimen length (mm)	f_y (N/mm ²)	f_{ck} (N/mm ²)	Steel ratio	Axial load (kN)	Age at loading (day)
120	450	315	26.8	0.148	300.0	28

Table 6(c) Details of CFT columns (example 5)

Steel tube outside diameter (mm)	Specimen length (mm)	f_y (N/mm ²)	f_{ck} (N/mm ²)	Steel ratio	Eccentricity (mm)	Age at loading (day)
120	450	315	26.8	0.148	16.8	28

Table 6(d) Details of CFT columns (example 6)

Steel tube outside diameter (mm)	Specimen length (mm)	f_y (N/mm ²)	f_{ck} (N/mm ²)	Steel ratio	Eccentricity (mm)	Axial load (kN)
120	450	315	26.8	0.148	16.8	300.0

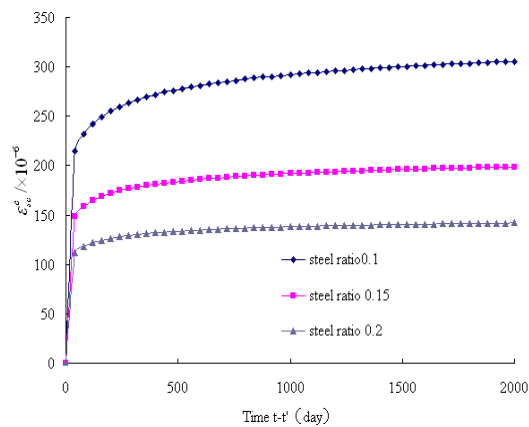


Fig. 7 Influence curves of steel ratio (example 3)

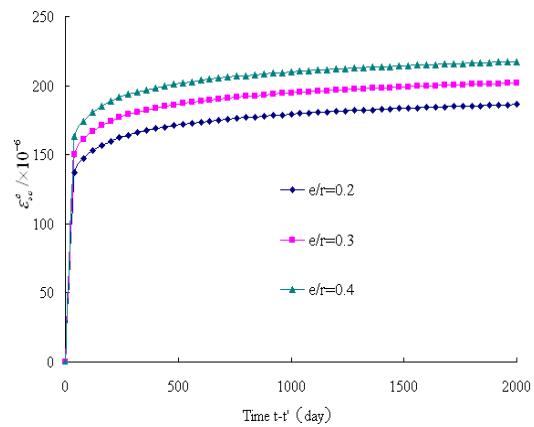


Fig. 8 Influence curves of eccentricity ratio (example 4)

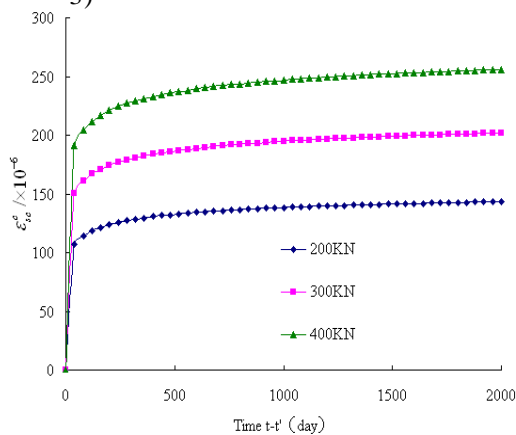


Fig. 9 Influence curves of axial load (example 5)

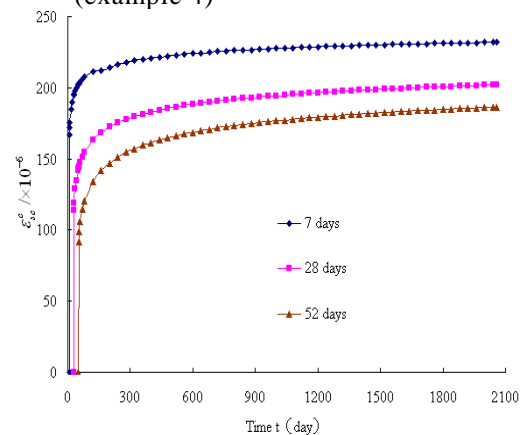


Fig. 10 Influence curves of concrete age at loading (example 6)

Figs. 7-10 are creep curves of the CFT columns with different steel ratio, eccentricity ratio, axial load and concrete age at loading when other parameters are the same. From these Figs. 7-10, following conclusions have been drawn:

- (1) With the increase of steel ratio, reduction of creep is observed. This is because steel ratio stands for the steel confinement to concrete. Creep develops when the confinement effect gets smaller. After 2000 days of loading, creep is reduced by 50%, when the steel ratio is increased from 0.1 to 0.2.
- (2) With the larger eccentricity is, the higher CFT creep is observed This is attributed to stress

distribution in the section which is considered to be related directly to eccentricity ratio. With bigger eccentricities, maximum stress on the section of CFT members will be higher, so that they creep more. When eccentricity increases from 0.2 to 0.4, creep increases by 16.7%.

(3) As axial load gets heavier, stress on the section will be larger, which makes creep strains also become larger. In example 5, when the axial load change from 200 kN to 400 kN, creep will increase by 78%.

(4) The later the members are loaded, the more concrete aging process is finished, which makes concrete stronger. As a result, creep strain will decrease. When the concrete age at loading is changed from 7 days to 52 days, observed creep reduction will be about 24.5%.

4. Conclusions

From the study presented in the paper, the following conclusions can be drawn:

(1) In the paper, we find creep of CFT columns under eccentric compressive loading develops quickly at the beginning. 80% of creep strain in 2000 days is completed within the first 500 days. After that, creep curves still trend upwards but at much slower rate.

(2) With increase in eccentricity, the creep in CFT columns is also increased. It is found that changing of eccentricity from 0.2 to 0.4, creep increases by 16.7%.

(3) Comparing with other model, the predicted creep results based on the Model B3 are more close to the experimental results, and differences between the theoretical and experimental curves are 10% approximately. In addition, the Model B3 can provide a more convenient approach to analyze effects of the internal factors on creep.

(4) Internal factors of concrete core, such as water to cement ratio and aggregate to cement ratio, do not significantly affect the creep of CFT columns. By contrast, the external factors, such as steel ratio and load level, have obvious effects on the creep of CFT columns.

Acknowledgments

The authors would like to gratefully acknowledge the financial support of National Science Foundation of China (Grant No. 50778020 and Grant No. 51078027).

References

- Ahmad, S.H. and Shah, S.P. (1982), "Complete triaxial stress-strain curves for concrete", *J. Struct. Div.*, **108**(4), 728-742.
- Bazant, Z.P. and Murphy, W.P. (1995), "Creep and shrinkage prediction model for analysis and design of concrete structures - model b3", *Mater. Struct.*, **28**(180), 357-365.
- Bazant, Z.P. and Prasannan, S. (1989a), "Solidification theory for concrete creep i. Formulation", *J. Eng. Mech.*, **115**(8), 1691-1703.
- Bazant, Z.P. and Prasannan, S. (1989b), "Solidification theory for concrete creep ii. Verification and application", *J. Eng. Mech.*, **115**(8), 1704-1725.
- Furlong, R.W. (1967), "Strength of steel-encased concrete beam-columns", *J. Struct. Div.*, **93**(5), 113-124.
- Gajalakshmi, P., Helena, H.J. and Raghavan, R.S. (2011), "Experimental investigation on the behaviour of concrete-filled steel columns", *Asian J. Civil Eng.*, **12**(6), 691-701.

- Han, L.H., Tao, Z. and Liu, W. (2004), "Effects of sustained load on concrete-filled hollow structural steel columns", *J. Struct. Eng.*, **130**(9), 1392-1404.
- Han, L.H. and Yang, Y.F. (2004), "The behavior of concrete-filled steel tubular columns with rectangular section under long-term loading", *China Civil Eng. J.*, **37**(3), 12-18. (in Chinese)
- Ichinose, L.H., Watanabe, E. and Nakai, H. (2001), "An experimental study on creep of concrete filled steel pipes", *J. Constr. Steel. Res.*, **57**(4), 453-466.
- Lam, J.P. (2002), *Evaluation of concrete shrinkage and creep prediction models*, San Jose, San Jose State University, Master.
- Morino, S., Kswaguchi, J. and Cao, Z.S. (1996), "Creep behavior of concrete-filled steel tubular members", *Proceedings of An engineering foundation conference on steel-concrete composite structures*, Irsee, Ger, ASCE, New York, NY, USA.
- Naguib, W. and Mirmiran, A. (2002), "Flexural creep tests and modeling of concrete-filled fiber reinforced polymer tubes", *J. Compos. Constr.*, **6**(4), 272-279.
- Naguib, W. and Mirmiran, A. (2003), "Creep modeling for concrete-filled steel tubes", *J. Constr. Steel. Res.*, **59**(11), 1327-1344.
- Nakai, H., Watanabe, E. and Ichinose, L.H. (1991). "An experimental study on creep of concrete filled steel pipes", *3rd international conference on steel-concrete composite structures*, Fukuoka, Japan.
- Neville, A.M., Dilger, W.H. and Brooks, J.J. (1983), *Creep of plain and structural concrete*, Construction Press, London and New York.
- Rajeev, G., Ram, K. and Paul, D.K. (2007), "Comparative study of various creep and shrinkage prediction models for concrete", *J. Mater. Civil Eng.*, **19**(3), 249-260.
- Shrestha, K.M., Chen, B.C. and Chen, Y.F. (2011), "State of the art of creep of concrete filled steel tubular arches", *KSCE J. Civil Eng.*, **15**(1), 145-151.
- Tan, S.J. and Qi, J.L. (1987), "The test research of strength of axially compressed cfst members under long-time loading", *Civil Eng. Architect.*, **20**(2), 10-24. (in Chinese)
- Uy, B. (2001), "Static long-term effects in short concrete-filled steel box columns under sustained loading", *ACI Struct. J.*, **98**(1), 96-104.
- Wang, Y.F. and Han B. (2007), "Creep analysis of concrete filled steel tube arch bridges", *Struct. Eng. Mech.*, **27**(6), 1-12.
- Wang, Y.F., Han, B. and Zhang, D.J. (2008). "Advances in creep of concrete filled steel tube members and structures", *Proceedings of the CONCREEP 8 conference (Creep, Shrinkage and Durability Mechanics of Concrete and Concrete Structures)*, Ise-Shima, Japan, Taylor & Francis.